Journal of Computational Physics 228 (2009) 8627–8641

Contents lists available at ScienceDirect

Journal of Computational Physics

journal homepage: www.elsevier.com/locate/jcp

Stokes–Darcy boundary integral solutions using preconditioners

Yassine Boubendir, Svetlana Tlupova *

Department of Mathematical Sciences and Center for Applied Mathematics and Statistics, New Jersey Institute of Technology, 323 Dr. Martin Luther King, Jr. Boulevard, University Heights, Newark, NJ 07102, USA

ARTICLE INFO

Article history:
Received 11 November 2008
Received in revised form 19 June 2009
Accepted 19 August 2009
Available online 28 August 2009

Keywords:
Preconditioner
Boundary integral method
Stokes flow
Darcy equations

ABSTRACT

In a system where a free fluid flow is coupled to flow in a porous medium, different PDEs are solved simultaneously in two subdomains. We consider steady Stokes equations in the free region, coupled across a fixed interface to Darcy equations in the porous substrate. Recently, the numerical solution of this system was obtained using the boundary integral formulation combined with a regularization-correction procedure. The correction process also results in the improvement of the condition number of the linear system. In this paper, an appropriate preconditioner based on the singular part of corrections is introduced to improve the convergence of a Krylov subspace method applied to solve the integral formulation.

Published by Elsevier Inc.

1. Introduction

We are interested in problems where a domain filled with fluid is separated by an interface from a porous medium filled with the same fluid. Systems like this have many important industrial applications [5,27,29]. We model the free fluid flow by the incompressible Stokes equations, and the flow in the porous medium by Darcy equations. The partial differential equations then have different orders in two subdomains and the coupling conditions at the interface have been investigated in various works [6,31,20,21,32]. Among these conditions are the continuity of normal components of velocity and normal stress, and the slip condition for the tangential velocity proposed by Beavers and Joseph [6]. Various numerical methods have been developed to solve this kind of problem (see, for instance [7,11,12,14,17,23–25,34]). In [34], a boundary integral formulation obtained using the free-space Green's function was used to represent solutions of both equations. Common advantages of this approach include reduction in the dimensionality of the problem and accuracy of solution. The boundary was represented as a distribution of singularities with strengths to be determined from the boundary and interface conditions. In addition, the authors in [34] applied a regularization-correction procedure to eliminate the singularities in the kernels and enhance the accuracy of the final solution. The resulting linear system was then solved by means of a Krylov subspace method (GMRES). This paper is devoted to the improvement of convergence of this method by using an appropriate preconditioner.

To eliminate the singularities that appear in the integral formulation, we regularize the kernels by approximating the delta function with a smooth radially symmetric function [9,34]. Then, a standard quadrature can be used to discretize this formulation. Numerical results have demonstrated that this technique results in low accuracy of the solution. As it was done in [34], we use the correction method to reduce the dependence of the numerical error on regularization. These corrections are based on the error due to regularization computed approximately near the singularity point. Precisely, it is defined as the difference between the original integral equations (singular kernels) and the ones with regularized kernels. The resulting

* Corresponding author.
E-mail address: svetlana.tlupova@njit.edu (S. Tlupova).

0021-9991/$ - see front matter Published by Elsevier Inc.
doi:10.1016/j.jcp.2009.08.014

integral representations for the fluid quantities are substituted into the boundary and interface conditions. The final integral equation system is then solved using a Krylov subspace method (GMRES) for the unknown force densities on the boundary. Initial observations showed that correction terms designed primarily to improve the accuracy of solution significantly reduce the condition numbers of the matrix. This also results in faster convergence rates using a Krylov subspace method, as some numerical tests illustrate in this paper.

The subject of present investigation concerns the improvement of the Krylov subspace method applied to the coupled Stokes–Darcy integral formulation. Indeed, the resulting linear system is non-symmetric and composed of dense blocks. Although the correction procedure considerably reduces the condition number, this linear system remains ill-conditioned, and its eigenvalues are largely clustered near zero. In addition to these disadvantages, the condition number increases with the number of grid points and the iterative method depends on the physical parameters, like fluid viscosity and permeability of the porous medium. The concept of the preconditioner introduced in this paper is based on the observation described above regarding the reduction of condition numbers when corrections are added. The technique consists of first introducing a matrix with a similar block structure as the Stokes–Darcy system. Then, for each block in this initial system we compute, using the singular part of corrections, the corresponding block in the new matrix. Its inverse finally defines our peconditioner, which can be solved efficiently since it has a small bandwidth. Indeed, the blocks of this matrix are either diagonal or have only a few non-zero off-diagonal elements. This strategy also suggests the possibility of using this type of preconditioner for problems where the solution can be expressed with similar Green's functions. We first present numerical results validating our approach for a Stokes flow problem. Then, we show numerical simulations corresponding to the Stokes–Darcy formulation, where significant improvement of GMRES using this preconditioner is demonstrated.

The paper is organized as follows. After the presentation of the model problem in Section 2, we describe the integral formulation and the regularization-correction technique in Section 3. In Section 4, we introduce the preconditioner, its derivation and overall structure. Finally, several numerical experiments validating our approach are presented in Section 5. Section 6 is reserved for conclusions.

2. Problem formulation

In situations where inertia has a negligible effect, the flow is modeled by the linear Stokes equations. In the porous substrate, we use Darcy's law which is a linear relationship between the driving pressure gradient and the filtration velocity. In two dimensions, we denote the Stokes domain by Ω_S and the Darcy one by Ω_D (Fig. 1). We assume bounded domains with smooth boundaries denoted by $\partial\Omega_S = \Gamma_S \cup \Sigma$ and $\partial\Omega_D = \Gamma_D \cup \Sigma$, where Σ is the common interface. The steady state equations are therefore given as follows:

$$\text{In}\,\Omega_S : \begin{cases} -\nabla p_S + \mu\Delta \mathbf{u}_S + \mathbf{F}_S = 0, \\ \nabla \cdot \mathbf{u}_S = 0, \end{cases} \tag{1}$$

where μ is the fluid dynamic viscosity, p_S is the pressure, $\mathbf{u}_S = (u_S, v_S)$ is the velocity vector, $\mathbf{F}_S$ is external force, and

$$\text{In}\,\Omega_D : \begin{cases} -\nabla p_D - \mu K^{-1}\mathbf{u}_D + \mathbf{G}_D = 0, \\ \nabla \cdot \mathbf{u}_D = 0, \end{cases} \tag{2}$$

where $\mathbf{u}_D = (u_D, v_D)$ and p_D are, respectively the (averaged) fluid velocity and the hydrostatic pressure, $\mathbf{G}_D$ is force, and K is the permeability of the porous medium. We will assume that the medium is isotropic, $K = kI$. Finally, we assume the following boundary conditions:

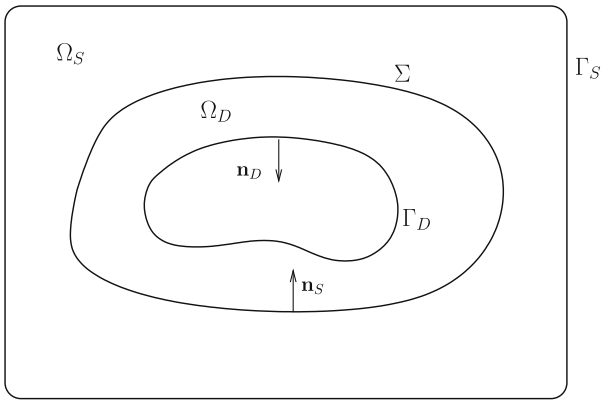

Fig. 1. Schematic of the problem.

$$\mathbf{u}_S = \mathbf{u}_0 \quad \text{on} \quad \Gamma_S, \tag{3}$$
$$p_D = p_0 \quad \text{on} \quad \Gamma_D, \tag{4}$$

and on Σ

$$\mathbf{u}_S \cdot \mathbf{n}_S = -\mathbf{u}_D \cdot \mathbf{n}_D, \tag{5}$$
$$p_S - 2\mu \mathbf{n}_S \cdot \mathbf{D}_S \cdot \mathbf{n}_S = p_D, \tag{6}$$
$$\frac{\partial u_S^{(\tau)}}{\partial \mathbf{n}_S} = \frac{\gamma}{\sqrt{k}} u_S^{(\tau)}. \tag{7}$$

Here γ is a dimensionless slip coefficient that depends on the geometry of the porous medium, $\mathbf{D}_S = \frac{1}{2}[\nabla \mathbf{u}_S + (\nabla \mathbf{u}_S)^T]$ is the Stokes deformation tensor, $u^{(\tau)}$ is the tangential velocity, and $\mathbf{n}_S$ (respectively, $\mathbf{n}_D$) is the unit normal vector that points out of the region Ω_D(respectively Ω_S), so that $\mathbf{n}_D = -\mathbf{n}_S$ on Σ. Eqs. (5) and (6) represent continuity of normal component of velocity and normal component of normal stress, and (7) is a slip condition of Beavers–Joseph–Saffman [6,31]. For detailed discussion on the coupling conditions, refer to [6,31,20,21,32].

3. Boundary integral formulation and regularization

The linearity of the problems makes the boundary integral equation method a natural approach to express solutions of various boundary value problems. The boundary integral formulation used in this paper provides representation of the flow in terms of primary variables, i.e., velocity, pressure, stress [28,19], as an alternative approach to the stream function formulation [15,16]. To derive the integral formulation, the governing Eqs. (1) and (2) are solved where the boundary is represented as a distribution of singular force [34,26]. Introducing a density $\mathbf{f}$ of the force distributed along the Stokes boundary and density $\mathbf{g}$ of the force along the Darcy boundary, we write

$$\mathbf{F}_S = \int_{\partial\Omega_S} \delta(\mathbf{x} - \mathbf{x}(s))\mathbf{f}(s)ds, \quad \mathbf{G}_D = \int_{\partial\Omega_D} \delta(\mathbf{x} - \mathbf{x}(s))\mathbf{g}(s)ds,$$

where s is a boundary parametrization, which we assume to be arclength for simplicity. Using the incompressibility conditions, both the Stokes and Darcy equations can be reduced to Laplace's equations for pressures. Once calculated, p_S and p_D are substituted into (1) and (2) to compute the velocities $\mathbf{u}_S$ and $\mathbf{u}_D$. The resulting expressions can be written as [9,34]

$$p_S(\mathbf{x}) = \int_{\partial\Omega_S} \nabla G(\mathbf{x} - \mathbf{x}(s)) \cdot \mathbf{f}(s)ds, \tag{8}$$
$$\mu \mathbf{u}_S(\mathbf{x}) = \int_{\partial\Omega_S} \{-G(\mathbf{x} - \mathbf{x}(s))\mathbf{f}(s) + \nabla[\nabla B(\mathbf{x} - \mathbf{x}(s))] \cdot \mathbf{f}(s)\}ds, \tag{9}$$

for Stokes and

$$p_D(\mathbf{x}) = \int_{\partial\Omega_D} \nabla G(\mathbf{x} - \mathbf{x}(s)) \cdot \mathbf{g}(s)ds, \tag{10}$$
$$\mu \mathbf{u}_D(\mathbf{x}) = -k \int_{\partial\Omega_D} \nabla[\nabla G(\mathbf{x} - \mathbf{x}(s))] \cdot \mathbf{g}(s)ds, \tag{11}$$

for Darcy quantities, where G and B are solutions of $\Delta G(\mathbf{x}) = \delta(\mathbf{x})$ and $\Delta B(\mathbf{x}) = G(\mathbf{x})$ in free-space defined by

$$G(\mathbf{x}) = \frac{1}{2\pi} \ln|\mathbf{x}|, \quad B(\mathbf{x}) = \frac{|\mathbf{x}|^2}{8\pi}(\ln|\mathbf{x}| - 1), \quad \mathbf{x} \in \mathbb{R}^2.$$

The formulation (8)–(11) provides the Stokes flow quantities in terms of a given boundary density $\mathbf{f}$, and the Darcy quantities in terms of a given density $\mathbf{g}$. Conversely, the unknowns $\mathbf{f}$ and $\mathbf{g}$ can be computed using boundary conditions on $\partial\Omega_S$ and $\partial\Omega_D$, respectively. Given the Stokes velocity for example, $\mathbf{f}$ can be found by solving an integral equation that results from evaluating (9) on the boundary, see [28,9,13] for a few examples of these techniques. In the coupled Stokes–Darcy problem, the system of integral equations for $\mathbf{f}$ and $\mathbf{g}$ is obtained by substituting (8)–(11) into the boundary and interface conditions (3)–(7). Once this system is solved, $\mathbf{f}$ can be substituted back into (8) and (9) to determine Stokes flow in Ω_S, and $\mathbf{g}$ can be substituted into (10) and (11) to compute the Darcy quantities in Ω_D.

Accurate computation of integrals (8)–(11) appears to be difficult when the evaluation point is near the boundary [3,2], and special techniques such as [18] can be used. A simple method for computing nearly singular integrals with higher accuracy that does not require a dense resolution was developed in [3], and used in the context of Stokes flow in [4,9]. This method is based on regularizing the integrands, applying a standard quadrature rule, and adding corrections for higher accuracy. The preconditioner proposed in this paper is based on ideas of the correction method used in [34] (see Section 3.1 for details).

In addition to the accuracy considerations, the mathematical representation (8)–(11) needs special treatment when evaluating the integrals on the boundary. The integral representation in (9) is continuous across the boundary $\partial\Omega_S$, but the integrals in (8), (10), (11) have limiting values different from the value on the boundary. Therefore, certain jump conditions have

to be incorporated into the solution of a boundary value problem. This issue also appears in conditions (6) and (7), since they require accurate evaluation of the velocity gradients at the interface.

The jump conditions in all these quantities can be found explicitly if the integrals are written as a superposition of a single and double layer potentials (see [34] for details):

$$w_0(\mathbf{x}) = V_0[\phi](\mathbf{x}) + N_0[\psi](\mathbf{x}), \quad \mathbf{x} \in \Omega, \tag{12}$$

where we have introduced a general quantity w_0 to represent the unknowns p and $\mathbf{u}$ for both flows, $V_0[\phi]$ and $N_0[\psi]$ are, respectively the single and the double layer potentials associated with continuous densities ϕ and ψ,

$$V_0[\phi](\mathbf{x}) := \int_{\partial\Omega} G(\mathbf{x} - \mathbf{x}(s))\phi(s)ds, \quad N_0[\psi](\mathbf{x}) := \int_{\partial\Omega} \nabla G(\mathbf{x} - \mathbf{x}(s)) \cdot \mathbf{n}(s)\psi(s)ds. \tag{13}$$

The single layer potential is continuous across the boundary $\partial\Omega$, and the double layer potential has a discontinuity equal to ψ across $\partial\Omega$ [8,22], so to evaluate (12) on the boundary we need to compute

$$w_0(\mathbf{x}) = V_0[\phi](\mathbf{x}) + N_0[\psi](\mathbf{x}) - \frac{1}{2}\psi(\mathbf{x}), \quad \mathbf{x} \in \partial\Omega. \tag{14}$$

In what follows, we explain briefly the regularization-correction method and present the derivation of the preconditioner we are proposing.

3.1. Regularization and correction

The main idea of the regularization procedure is to compute the regularized Green's function from $\Delta G_\delta(\mathbf{x}) = \xi_\delta(\mathbf{x})$, where ξ_δ is a smooth function that approximates the delta function and satisfies $\int \xi_\delta(\mathbf{x})d\mathbf{x} = \int \delta(\mathbf{x})d\mathbf{x} = 1$. We use the smoothing function from [34]:

$$\xi_\delta(\mathbf{x}) = \frac{2\delta^4}{\pi(|\mathbf{x}|^2 + \delta^2)^3}, \tag{15}$$

where the parameter δ is chosen according to accuracy constraints. The corresponding regularized Green's function is

$$G_\delta(\mathbf{x}) = \frac{1}{4\pi}\left[\ln(|\mathbf{x}|^2 + \delta^2) - \frac{\delta^2}{|\mathbf{x}|^2 + \delta^2}\right],$$

so that $G_\delta \to G$ as $\delta \to 0$. This regularization method for Stokes flow was proposed in [9] and further investigated in applications in [10,13,1]. Fig. 2 shows the Green's function for different values of regularization parameter δ, where $\delta = 0$ is the singular case. As can be seen from the figure, the largest approximation is made near the singularity $|\mathbf{x}| = 0$. Away from the singularity we have

$$(G - G_\delta)(\mathbf{x}) = O\left(\frac{\delta^4}{|\mathbf{x}|^4}\right) \quad \text{for} \quad \delta \ll |\mathbf{x}|. \tag{16}$$

This observation suggests that the approximation can be improved by considering the error near the singularity. When computing (12), regularization introduces an error of the form

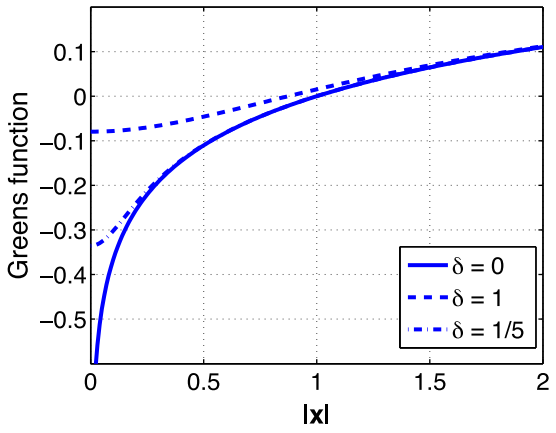

Fig. 2. Green's function for different values of δ.

$$(w_0 - w_\delta)(\mathbf{x}) = \int_{\partial\Omega} (G - G_\delta)(\mathbf{x} - \mathbf{x}(s))\phi(s)ds + \int_{\partial\Omega} \nabla(G - G_\delta)(\mathbf{x} - \mathbf{x}(s)) \cdot \mathbf{n}(s)\psi(s)ds = (V_0 - V_\delta)[\phi](\mathbf{x}) + (N_0 - N_\delta)[\psi](\mathbf{x}),$$

where $V_\delta[\phi]$ and $N_\delta[\psi]$ are defined as in (13) with G replaced by G_δ. The leading error term can be identified by expanding the smooth functions $\phi(s)$ and $\psi(s)$ in Taylor series around the point $\mathbf{x}(s^*)$ that is closest to $\mathbf{x}$:

$$\phi(s) = \phi(s^*) + \phi_s(s^*)(s - s^*) + O((s - s^*)^2),$$
$$\psi(s) = \psi(s^*) + \psi_s(s^*)(s - s^*) + O((s - s^*)^2),$$

for s near s^*, and keeping only the first term in the expansions,

$$\begin{aligned}(w_0 - w_\delta)^*(\mathbf{x}) &= \int_{\partial\Omega} (G - G_\delta)(\mathbf{x} - \mathbf{x}(s))ds \cdot \phi(s^*) + \int_{\partial\Omega} \nabla(G - G_\delta)(\mathbf{x} - \mathbf{x}(s)) \cdot \mathbf{n}(s)ds \cdot \psi(s^*) \\ &= (V_0 - V_\delta)^*[\phi](\mathbf{x}) + (N_0 - N_\delta)^*[\psi](\mathbf{x}),\end{aligned} \tag{17}$$

where $V^*[\phi] \equiv V[\phi(s^*)], N^*[\psi] \equiv N[\psi(s^*)]$. These terms are then added as corrections to increase the accuracy, so the fluid quantities are computed as follows:

$$w(\mathbf{x}) = w_\delta(\mathbf{x}) + (w_0 - w_\delta)^*(\mathbf{x}) = V_\delta[\phi](\mathbf{x}) + N_\delta[\psi](\mathbf{x}) + \left[I^G(\mathbf{x}) - I^G_\delta(\mathbf{x})\right]\phi(s^*) - \left[1 - I^{(n)}_\delta(\mathbf{x})\right]\psi(s^*), \tag{18}$$

where

$$I^{(n)}_\delta(\mathbf{x}) = -\int_{\partial\Omega} \nabla G_\delta(\mathbf{x} - \mathbf{x}(s)) \cdot \mathbf{n}(s)ds, \tag{19}$$

$$I^G(\mathbf{x}) = \int_{\partial\Omega} G(\mathbf{x} - \mathbf{x}(s))ds, \tag{20}$$

$$I^G_\delta(\mathbf{x}) = \int_{\partial\Omega} G_\delta(\mathbf{x} - \mathbf{x}(s))ds, \tag{21}$$

and we have used the identity

$$\int_{\partial\Omega} \nabla G(\mathbf{x} - \mathbf{x}(s)) \cdot \mathbf{n}(s)ds = -1, \quad \mathbf{x} \in \Omega.$$

Eq. (18) is valid on the boundary as well, since the jump condition in the double layer is added due to

$$I^{(n)}_\delta(\mathbf{x}) \approx \begin{cases} 1, & \mathbf{x} \in \Omega, \\ 1/2, & \mathbf{x} \in \partial\Omega. \end{cases}$$

The correction is also beneficial when the evaluation point is off the boundary, but near it. Let us point out that the accuracy can be further improved by using the method developed in [3] for the single and double layer potentials, where corrections for the regularization and discretization errors were derived. In the remainder of this Section, we give the regularized formulation for Stokes, Darcy, and the coupled system.

3.2. Stokes solution

The regularization-correction technique described above is applied to solve the Stokes–Darcy problem (1)–(7). The details of the derivation are given in [34]. Here, we summarize the principal equations used to solve the problem. The integrals (8)–(11) are first modified to be in the form of potentials (12) by using the following decomposition

$$\mathbf{f}(s) = f^{(n)}(s)\mathbf{n}(s) + f^{(\tau)}(s)\boldsymbol{\tau}(s), \tag{22}$$

of the unknown force distributed along the Stokes boundary, where $\boldsymbol{\tau}(s) = (x_s(s), y_s(s))$ and $\mathbf{n}(s) = (y_s(s), -x_s(s))$ are, respectively the unit tangential and outward normal vectors at arclength s. Substituting this into (8), the Stokes pressure becomes

$$p_S(\mathbf{x}) = V_0[f^{(\tau)}_s(s)](\mathbf{x}) + N_0[f^{(n)}(s)](\mathbf{x}), \tag{23}$$

where the single layer was obtained using integration by parts. Similarly, the Stokes velocity can be written in terms of potentials as [9,34]

$$\mathbf{u}_S(\mathbf{x}) = V_0[\boldsymbol{\Phi}(s)](\mathbf{x}) + N_0[\boldsymbol{\Psi}(s)](\mathbf{x}), \tag{24}$$

where

$$\boldsymbol{\Phi}(s) = (\Phi_1, \Phi_2)(s) = -\frac{\mathbf{f}(s)}{2\mu} + \left[\frac{\mathbf{x} - \mathbf{x}(s)}{2\mu} f^{(\tau)}(s)\right]_s, \quad \boldsymbol{\Psi}(s) = (\Psi_1, \Psi_2)(s) = \frac{\mathbf{x} - \mathbf{x}(s)}{2\mu} f^{(n)}(s), \tag{25}$$

with $(\cdot)_s = d(\cdot)/ds$. Notice that when $\mathbf{x} \in \partial\Omega_S$, (23) needs to be modified similarly to (14), whereas (24) becomes a single layer potential since $\boldsymbol{\Psi}(s^*) = 0$ on the boundary.

In a coupled Stokes–Darcy problem, the interface conditions (6) and (7) require accurate computation of the matrix

$$\nabla \mathbf{u}_S = \begin{pmatrix} \frac{\partial u}{\partial x} & \frac{\partial u}{\partial y} \\ \frac{\partial v}{\partial x} & \frac{\partial v}{\partial y} \end{pmatrix}.$$

Each of the four components can be written in a similar form using the fact that derivatives of potentials can be computed as potentials. To compute $\frac{\partial u_S}{\partial y}(\mathbf{x})$, for example, the first component in (24) is differentiated using

$$\frac{\partial}{\partial y} V_0[\phi](\mathbf{x}) = V_0[(\phi y_s)_s](\mathbf{x}) - N_0[\phi x_s](\mathbf{x}), \quad \frac{\partial}{\partial y} N_0[\psi](\mathbf{x}) = V_0[(\psi x_s)_s](\mathbf{x}) + N_0[\psi y_s](\mathbf{x}),$$

with densities ϕ and ψ given by (24), to obtain the following representation for $\mathbf{x} \in \Omega_S$:

$$\frac{\partial u_S}{\partial y}(\mathbf{x}) = V_0\left[\{\Phi_1(s) y_s(s) + \Psi_{1s}(s) x_s(s)\}_s\right](\mathbf{x}) - N_0[\{\Phi_1(s) x_s(s) - \Psi_{1s}(s) y_s(s)\}](\mathbf{x}), \tag{26}$$

where $\Psi_{1s} = d\Psi_1/ds$. If $\mathbf{x} \in \partial\Omega_S$, this expression has to be modified to take into consideration the jump conditions arising from the double layer, see [34,33] for details and results.

We apply the regularization-correction technique (Section 3.1) to compute Stokes flow by evaluating the fluid quantities (23)–(26) as in (18). Notice that the unknown $\mathbf{f}$ is given in integrals in differentiated form. By using integration by parts, the integrals simplify to the following final expressions where the density $\mathbf{f}$ appears readily [34,33]:

$$p_S(\mathbf{x}) = \int_{\partial\Omega_S} \nabla G_\delta(\mathbf{x} - \mathbf{x}(s)) \cdot \mathbf{f}(s) ds + \Delta I^n(\mathbf{x}) f^{(n)}(s^*) + \Delta I^G(\mathbf{x}) f_s^{(\tau)}(s^*), \tag{27}$$

$$\mathbf{u}_S(\mathbf{x}) = \int_{\partial\Omega_S} \left\{ -G_\delta(\mathbf{x} - \mathbf{x}(s)) \frac{\mathbf{f}(s)}{2\mu} + \nabla G_\delta(\mathbf{x} - \mathbf{x}(s)) \cdot \mathbf{f}(s) \frac{\mathbf{x} - \mathbf{x}(s)}{2\mu} \right\} ds + \Delta I^G(\mathbf{x}) \mathbf{\Phi}(s^*), \tag{28}$$

$$\begin{aligned} \nabla \mathbf{u}_S(\mathbf{x}) = \int_{\partial\Omega_S} \Bigg\{ & -\frac{\mathbf{f}^T(s)}{2\mu} \nabla G_\delta(\mathbf{x} - \mathbf{x}(s)) + \frac{(\mathbf{x} - \mathbf{x}(s))^T}{2\mu} \nabla [\nabla G_\delta(\mathbf{x} - \mathbf{x}(s)) \cdot \mathbf{f}(s)] \\ & - \frac{(\mathbf{x} - \mathbf{x}(s))^T}{2\mu} f^{(n)}(s) \mathbf{n}(s) \xi_\delta(\mathbf{x} - \mathbf{x}(s)) + \frac{1}{2\mu} [\nabla G_\delta(\mathbf{x} - \mathbf{x}(s)) \cdot \mathbf{f}(s)] I \Bigg\} ds \\ & + \Delta I^G(\mathbf{x}) \left[\mathbf{\Phi}^T \boldsymbol{\tau} - \mathbf{\Psi}_s^T \mathbf{n} + \frac{f^{(\tau)}}{2\mu} I \right]_s (s^*) + \Delta I^n(\mathbf{x}) \left[\mathbf{\Phi}^T \mathbf{n} + \mathbf{\Psi}_s^T \boldsymbol{\tau} + \frac{f^{(n)}}{2\mu} I \right] (s^*), \end{aligned} \tag{29}$$

where $\mathbf{x} \in \partial\Omega_S, I$ is the 2×2 identity matrix, and ξ_δ is given by (15). All vectors in (29) are given in the row form, and $(\cdot)^T$ describes the transpose. Each component of (29) is computed similarly to (26). Here we have defined

$$\Delta I^n(\mathbf{x}) = -\left[1 - I_\delta^{(n)}(\mathbf{x})\right], \tag{30}$$

$$\Delta I^G(\mathbf{x}) = I^G(\mathbf{x}) - I_\delta^G(\mathbf{x}), \tag{31}$$

with $I_\delta^{(n)}, I^G$, and I_δ^G given by (19)–(21). These represent correction terms for the single and double layer potentials, respectively. The Stokes pressure p_S, for example, is computed as a combination of two potentials, and therefore has corrections for both. The velocity, on the other hand, has the correction term for the single layer potential alone on the boundary. For a shorthand notation, we write (27)–(29) as

$$p_S(\mathbf{x}) = \mathcal{K}_{\delta c}^p(\mathbf{x}) * \mathbf{f}, \quad \mathbf{u}_S(\mathbf{x}) = \mathcal{K}_{\delta c}^{\mathbf{u}}(\mathbf{x}) * \mathbf{f}, \quad \frac{\partial u_S^{(\tau)}}{\partial \mathbf{n}_S} = \mathcal{K}'_{\delta c}(\mathbf{x}) * \mathbf{f}, \quad \mathbf{n}_S \cdot \mathbf{D}_S \cdot \mathbf{n}_S = \mathcal{K}''_{\delta c}(\mathbf{x}) * \mathbf{f}, \tag{32}$$

where $\mathbf{f} = (f^{(\tau)}, f^{(n)})^T, \mathbf{D}_S$ is the Stokes deformation tensor, and the subscript δc indicates the regularization-correction procedure.

3.3. Darcy solution

Using a decomposition similar to (22) for the force $\mathbf{g}$ along the boundary $\partial\Omega_D$,

$$\mathbf{g}(s) = g^{(n)}(s) \mathbf{n}(s) + g^{(\tau)}(s) \boldsymbol{\tau}(s), \tag{33}$$

the Darcy pressure can be written as

$$p_D(\mathbf{x}) = V_0\left[g_s^{(\tau)}(s)\right] + N_0[g^{(n)}(s)]. \tag{34}$$

To derive a similar form for the velocity, potentials in Eq. (34) are differentiated using the Darcy Eq. (2) to give [34]

$$\mathbf{u}_D(\mathbf{x}) = -\frac{\kappa}{\mu} V_0\left[\left(g_s^{(\tau)}(s)\boldsymbol{\tau}(s) - g_s^{(n)}(s)\mathbf{n}(s)\right)_s\right] - \frac{\kappa}{\mu} N_0\left[g_s^{(\tau)}(s)\mathbf{n}(s) + g_s^{(n)}(s)\boldsymbol{\tau}(s)\right]. \tag{35}$$

This is a general formulation to determine the Darcy flow from two force components on the boundary, $g^{(\tau)}$ and $g^{(n)}$. Notice that only one of these components can be determined from the given boundary and interface conditions. To match the unknowns with the conditions, we assume that the Darcy force is normal to the boundary, i.e., $g^{(\tau)} \equiv 0$.

The method of regularization with corrections is again used for Darcy quantities (34) and (35) by applying the method of (18). After some algebra that involves simple integration by parts, the following expressions were obtained [34,33]:

$$p_D(\mathbf{x}) = \int_{\partial\Omega_D} \nabla G_\delta(\mathbf{x} - \mathbf{x}(s)) \cdot \mathbf{n}(s) g^{(n)}(s) ds + \Delta I^n(\mathbf{x}) g^{(n)}(s^*), \tag{36}$$

$$\begin{aligned}\mathbf{u}_D(\mathbf{x}) = -\frac{k}{\mu}\Big\{ &\int_{\partial\Omega_D} \left\{-\xi_\delta(\mathbf{x} - \mathbf{x}(s)) g^{(n)}(s)\mathbf{n}(s) + \nabla[\nabla G_\delta(\mathbf{x} - \mathbf{x}(s))] \cdot \mathbf{n}(s) g^{(n)}(s)\right\} ds \\ &+ \Delta I^n(\mathbf{x})\left[g_s^{(n)}(s)\boldsymbol{\tau}(s)\right]|_{s=s^*} - \Delta I^G(\mathbf{x})\left[g_s^{(n)}(s)\mathbf{n}(s)\right]_s|_{s=s^*}\Big\},\end{aligned} \tag{37}$$

where $\mathbf{x} \in \partial\Omega_D, \Delta I^n, \Delta I^G$ were defined in (30) and (31), and as before, ξ_δ is given by (15). Similarly to the Stokes quantities (32), we write Eqs. (36) and (37) as

$$p_D(\mathbf{x}) = \mathcal{H}^p_{\delta c}(\mathbf{x}) * \mathbf{g}, \quad \mathbf{u}_D(\mathbf{x}) = \mathcal{H}^{\mathbf{u}}_{\delta c}(\mathbf{x}) * \mathbf{g}, \tag{38}$$

where $\mathbf{g} = g^{(n)}$.

3.4. Coupled system

In the coupled Stokes–Darcy problem, the expressions for both fluid quantities (27)–(29), (36), (37) are combined to compute the unknown force densities $\mathbf{f}$ and $\mathbf{g}$ by satisfying the boundary and interface conditions (3)–(7). With the notation introduced in (32) and (38), enforcing continuity of normal velocity (5) on the interface gives

$$\left(\mathcal{K}^{\mathbf{u}}_{\delta c} \cdot \mathbf{n}_S\right)(\mathbf{x}) * \mathbf{f} = -(\mathcal{H}^{\mathbf{u}}_{\delta c} \cdot \mathbf{n}_D)(\mathbf{x}) * \mathbf{g}, \quad \mathbf{x} \in \Sigma. \tag{39}$$

Other conditions in (3)–(7) are imposed similarly. Then solving the coupled problem involves first solving the following linear system to satisfy the boundary and interface conditions (3)–(7):

$$(SD)F = b, \tag{40}$$

where

$$(SD) = \begin{pmatrix} \mathcal{K}^{\mathbf{u}}_{\delta c}|_{\Gamma_S} & 0 \\ \left(\mathcal{K}^{\mathbf{u}}_{\delta c} \cdot \mathbf{n}_S\right)|_\Sigma & \left(\mathcal{H}^{\mathbf{u}}_{\delta c} \cdot \mathbf{n}_D\right)|_\Sigma \\ \left(\mathcal{K}^p_{\delta c} - 2\mu\mathcal{K}''_{\delta c}\right)|_\Sigma & -\mathcal{H}^p_{\delta c}|_\Sigma \\ \left(\mathcal{K}'_{\delta c} - \frac{\gamma}{\sqrt{\kappa}}\mathcal{K}^{\mathbf{u}}_{\delta c} \cdot \tau_S\right)\Big|_\Sigma & 0 \\ 0 & \mathcal{H}^p_{\delta c}|_{\Gamma_D} \end{pmatrix}, \quad F = \begin{pmatrix} \mathbf{f} \\ \mathbf{g} \end{pmatrix}, \quad b = \begin{pmatrix} \mathbf{u}_0|_{\Gamma_S} \\ 0 \\ 0 \\ 0 \\ p_0|_{\Gamma_D} \end{pmatrix} \tag{41}$$

Observe that the non-symmetric matrix of this linear system is composed of dense blocks (from integrals with different kernels). Numerical tests performed in [34] show the accuracy improvement when using corrections. Another important observation is the reduction of the condition numbers. Indeed, without corrections, these numbers grow exponentially when increasing the regularization parameter δ [34]. Adding corrections improves the matrix condition numbers and convergence of the iterative technique. This will be illustrated in a Stokes flow example in a bounded domain, where we also show a significant increase of the convergence speed of GMRES using the preconditioner presented in this paper.

4. Preconditioner

As mentioned, the correction process improves the efficiency of the iterative technique to solve the linear system. From these results and observations, we propose a preconditioner for the system (41) provided by the correction terms. We first describe the general case of potentials. We write (18) as

$$w(\mathbf{x}) = \mathcal{P}_{\delta c}[\phi;\psi] = \mathcal{P}_\delta[\phi;\psi] + \mathcal{P}^*[\phi;\psi] - \mathcal{P}^*_\delta[\phi;\psi], \tag{42}$$

where $\mathcal{P}_\delta, \mathcal{P}^*, \mathcal{P}^*_\delta$ represent the integrals, the singular and the regularized parts of corrections in (18), respectively. With this notation, the preconditioner for $\mathcal{P}_{\delta c}$ is defined as

$$\widetilde{\mathcal{P}} = (\mathcal{P}^*)^{-1}. \tag{43}$$

Applying this preconditioner to w, we get

$$\widetilde{\mathcal{P}}\mathcal{P}_{\delta c}[\phi;\psi] = \left(\widetilde{\mathcal{P}}\mathcal{P}_{\delta} + \widetilde{\mathcal{P}}\mathcal{P}^{*} - \widetilde{\mathcal{P}}\mathcal{P}^{*}_{\delta}\right)[\phi;\psi] = (I-\Delta)[\phi;\psi], \tag{44}$$

where $\Delta = \widetilde{\mathcal{P}}(\mathcal{P}^{*}_{\delta} - \mathcal{P}_{\delta})$ depends on the regularization parameter δ with a property that $\Delta[\phi^{*},\psi^{*}] = 0$. This preconditioner corresponds to (18), which is a superposition of a single and double layers. The same approach will be used to construct the preconditioner, noted here by $((SD)^{*})^{-1}$, for the Stokes–Darcy problem (41). The matrix $(SD)^{*}$, which has the same structure as (SD), is obtained by computing the corresponding $\mathcal{P}^{*}$ for each block in (SD). For the sake of simplicity, we present in the next subsection the preconditioner in the context of Stokes velocity. Then, we show the structure and the elements of the preconditioner for the coupled system.

4.1. Stokes velocity

Consider Stokes flow in a domain Ω_S where the velocity of the fluid is given on the boundary:

$$-\nabla p_S + \mu\Delta\mathbf{u}_S + \mathbf{F}_S = 0, \quad \nabla\cdot\mathbf{u}_S = 0, \quad \mathbf{x}\in\Omega_S, \tag{45}$$

$$\mathbf{u}_S = \mathbf{u}_0 \quad \mathbf{x}\in\partial\Omega_S. \tag{46}$$

We use the representation (28) of the solution and evaluate it on the boundary $\mathbf{x}\in\partial\Omega_S$ to get

$$\mathbf{u}_S(\mathbf{x}) = \mathcal{K}^{\mathbf{u}}_{\delta c} * \mathbf{f} = \mathcal{K}^{\mathbf{u}}_{\delta}[f^{(\tau)};f^{(n)}] + (\mathcal{K}^{\mathbf{u}})^{*}[f^{(\tau)};f^{(n)}] - \left(\mathcal{K}^{\mathbf{u}}_{\delta}\right)^{*}[f^{(\tau)};f^{(n)}],$$

where the unknown density components for each operator are shown in square brackets $[\ ;\ ]$, so that

$$\mathcal{K}^{\mathbf{u}}_{\delta}[f^{(\tau)};f^{(n)}] = \int_{\partial\Omega_S}\left\{-G_{\delta}(\mathbf{x}-\mathbf{x}(s))\frac{\mathbf{f}(s)}{2\mu} + \nabla G_{\delta}(\mathbf{x}-\mathbf{x}(s))\cdot\mathbf{f}(s)\frac{\mathbf{x}-\mathbf{x}(s)}{2\mu}\right\}ds,$$

$$(\mathcal{K}^{\mathbf{u}})^{*}[f^{(\tau)};f^{(n)}] = I^{G}(\mathbf{x})\left\{-\frac{\boldsymbol{\tau}(s^{*})}{\mu}f^{(\tau)}(s^{*}) - \frac{\mathbf{n}(s^{*})}{2\mu}f^{(n)}(s^{*})\right\},$$

$$(\mathcal{K}^{\mathbf{u}}_{\delta})^{*}[f^{(\tau)};f^{(n)}] = I^{G}_{\delta}(\mathbf{x})\left\{-\frac{\boldsymbol{\tau}(s^{*})}{\mu}f^{(\tau)}(s^{*}) - \frac{\mathbf{n}(s^{*})}{2\mu}f^{(n)}(s^{*})\right\},$$

with I^{G}, I^{G}_{δ} given by (20) and (21). Without using a preconditioner, enforcing condition (46) results in solving

$$\mathcal{K}^{\mathbf{u}}_{\delta c}\mathbf{f} = \mathbf{u}_0, \tag{47}$$

for the unknown forces $\mathbf{f} = (f^{(\tau)},f^{(n)})^{T}$. On the other hand, to improve the convergence properties of the iterative technique, we solve Eq. (46) as

$$\widetilde{\mathcal{K}}\mathcal{K}^{\mathbf{u}}_{\delta c}\mathbf{f} = \widetilde{\mathcal{K}}\mathbf{u}_0, \tag{48}$$

with the preconditioner defined as

$$\widetilde{\mathcal{K}} = ((\mathcal{K}^{\mathbf{u}})^{*})^{-1} = \begin{pmatrix} D^{(\tau)}_{u} & D^{(n)}_{u} \\ D^{(\tau)}_{v} & D^{(n)}_{v}\end{pmatrix}^{-1}. \tag{49}$$

Each of the four blocks of the matrix $(\mathcal{K}^{\mathbf{u}})^{*}$ is a diagonal matrix with the elements equal to the coefficients of the forces in the corresponding component of velocity $\mathbf{u} = (u,v)$:

$$D^{(\tau)}_{u} = -\frac{\tau_1(s^{*})}{\mu}I^{G}(\mathbf{x}), \quad D^{(n)}_{u} = -\frac{n_1(s^{*})}{2\mu}I^{G}(\mathbf{x}),$$

$$D^{(\tau)}_{v} = -\frac{\tau_2(s^{*})}{\mu}I^{G}(\mathbf{x}), \quad D^{(n)}_{v} = -\frac{n_2(s^{*})}{2\mu}I^{G}(\mathbf{x}),$$

$\boldsymbol{\tau} = (\tau_1,\tau_2)$, $\mathbf{n} = (n_1,n_2)$, and $\mathbf{x} = \mathbf{x}(s^{*})$. Due to the block-diagonal structure of $(\mathcal{K}^{\mathbf{u}})^{*}$, the inverse can be computed easily. In the Numerical results section, we present experiments that show improvement of GMRES for this problem when solving the preconditioned system (48) instead of (47).

4.2. Coupled system

As mentioned, the same method is applied to derive the preconditioner for the coupled Stokes–Darcy system (41). The matrix $(SD)^{*}$ based on the singular part of corrections has the same block structure as (41):

$$(SD)^{*} = \begin{pmatrix} (\mathcal{K}^{\mathbf{u}})^{*} & 0 \\ (\mathcal{K}^{\mathbf{u}}\cdot\mathbf{n}_S)^{*} & (\mathcal{H}^{\mathbf{u}}\cdot\mathbf{n}_D)^{*} \\ (\mathcal{K}^{p} - 2\mu\mathcal{K}'')^{*} & -(\mathcal{H}^{p})^{*} \\ (\mathcal{K}')^{*} - \frac{\gamma}{\sqrt{\kappa}}(\mathcal{K}^{\mathbf{u}}\cdot\boldsymbol{\tau}_S)^{*} & 0 \\ 0 & (\mathcal{H}^{p})^{*}\end{pmatrix}, \tag{50}$$

where

$$(\mathcal{K}^p)^*[f^{(\tau)};f^{(n)}] = I^G(\mathbf{x})f_s^{(\tau)}(s^*) - f^{(n)}(s^*), \tag{51}$$

$$(\mathcal{K}^{\mathbf{u}})^*[f^{(\tau)};f^{(n)}] = I^G(\mathbf{x})\mathbf{\Phi}(s^*) - \mathbf{\Psi}(s^*) = I^G(\mathbf{x})\left\{-\frac{\mathbf{f}(s^*)}{2\mu} - \frac{\mathbf{x}_s(s^*)}{2\mu}f^{(\tau)}(s^*)\right\}, \tag{52}$$

$$(\mathcal{K}')^*[f^{(\tau)};f^{(n)}] = \boldsymbol{\tau}(s^*)\cdot\left[I^G(\mathbf{x})M_1(s^*) - M_2(s^*)\right]\cdot\mathbf{n}(s^*), \tag{53}$$

$$(\mathcal{K}'')^*[f^{(\tau)};f^{(n)}] = \mathbf{n}(s^*)\cdot\frac{1}{2}\left[I^G(\mathbf{x})\left(M_1 + M_1^T\right)(s^*) - \left(M_2 + M_2^T\right)(s^*)\right]\cdot\mathbf{n}(s^*), \tag{54}$$

$$(\mathcal{H}^p)^*[g^{(n)}] = -g^{(n)}(s^*), \tag{55}$$

$$(\mathcal{H}^{\mathbf{u}})^*[g^{(n)}] = -\frac{k}{\mu}\left\{I^G(\mathbf{x})\left[-g_s^{(n)}(s)\mathbf{n}(s)\right]_s|_{s=s^*} - \left[g_s^{(n)}(s)\boldsymbol{\tau}(s)\right]|_{s=s^*}\right\}, \tag{56}$$

where $I^G(\mathbf{x})$ is defined in (20), and $I^GM_1 - M_2$ represents the singular part of corrections for the matrix $\nabla\mathbf{u}_S$, with

$$M_1(s) = \frac{d}{ds}\left[\mathbf{\Phi}^T\boldsymbol{\tau} - \mathbf{\Psi}_s^T\mathbf{n} + \frac{f^{(\tau)}}{2\mu}I\right](s), \quad M_2(s) = \left[\mathbf{\Phi}^T\mathbf{n} + \mathbf{\Psi}_s^T\boldsymbol{\tau} + \frac{f^{(n)}}{2\mu}I\right](s),$$

where I is the identity matrix and using the notation of (25). Then the coefficients of $f^{(\tau)}, f^{(n)}$, and $g^{(n)}$ form the elements of $(SD)^*$.

5. Numerical results

5.1. Discretization

The numerical accuracy of solutions depends on the regularization parameter δ and the discretization quadrature. The interval $0 \leqslant s \leqslant L$ is discretized by $i = 1,\ldots,N$ grid points with spacing Δs_i. Once the kernels are regularized and all integrands are smooth functions, we use the trapezoidal rule

$$\int_0^L K_\delta(\mathbf{x} - \mathbf{x}(s))f(s)ds \approx \sum_{i=1}^{N} K_\delta(\mathbf{x} - \mathbf{x}(s_i))f(s_i)\Delta s_i,$$

to approximate the integrals in (27)–(29), (36), (37), including the integrals for $I_\delta^{(n)}(\mathbf{x})$ and $I_\delta^G(\mathbf{x})$ in (19) and (21). For accuracy estimates and improvements, see [3]. Higher-order integration techniques such as Gaussian quadrature could be used. However, it does not change the dependence of solutions on regularization when δ is large, and better accuracy is achieved only for smaller values of δ (see [34]). To compute $I^G(\mathbf{x})$ with better accuracy than trapezoidal rule, we use Gaussian quadrature.

With this discretization, the block matrices of system (50) have diagonal elements of the form

$$(\mathcal{K}^p)_{ii}^*[f^{(\tau)};f^{(n)}] = I^G(\mathbf{x}_i)f_s^{(\tau)}(s_i) - f^{(n)}(s_i),$$

for each point $\mathbf{x}_i = \mathbf{x}(s_i)$ on the boundary. The elements of $(\mathcal{K}^{\mathbf{u}})^*, (\mathcal{K}')^*, (\mathcal{K}'')^*, (\mathcal{H}^p)^*$, and $(\mathcal{H}^{\mathbf{u}})^*$ are computed similarly. Notice that terms of the form $cY(s_i)$, with Y representing $f^{(\tau)}, f^{(n)}$, or $g^{(n)}$, will form the diagonal elements of the particular block matrix in (50). If the term has the form $cY_s(s_i)$ or $cY_{ss}(s_i)$, then a few off-diagonal elements become non-zero, depending on the particular approximation of Y_s and Y_{ss} used. Therefore, the matrix $(SD)^*$ in (50) will have a block-diagonal or near diagonal structure and can be solved efficiently.

5.2. Cubic splines

To ensure smoothness, the boundary and the force distributions are parametrized using cubic splines:

$$\mathbf{x} = (x,y) = \mathbf{a}_k + \mathbf{b}_k(\alpha - \alpha_k) + \mathbf{c}_k(\alpha - \alpha_k)^2 + \mathbf{d}_k(\alpha - \alpha_k)^3,$$
$$Y(\alpha) = a_k + b_k(\alpha - \alpha_k) + c_k(\alpha - \alpha_k)^2 + d_k(\alpha - \alpha_k)^3,$$

for $\alpha_k \leqslant \alpha \leqslant \alpha_{k+1}, k = 1,\ldots,N$, with periodic boundary conditions, Y representing $f^{(\tau)}$, $f^{(n)}$, or $g^{(n)}$. The arclength $s = s(\alpha)$ is a smooth map with $ds/d\alpha = |d\mathbf{x}/d\alpha|$, so that $\frac{d(\cdot)}{ds} = \frac{d(\cdot)}{d\alpha}/\left|\frac{d\mathbf{x}}{d\alpha}\right|$. The unit tangent and normal vectors are $\boldsymbol{\tau}(\alpha) = T(\alpha)/|T(\alpha)|$, $\mathbf{n}(\alpha) = N(\alpha)/|N(\alpha)|$, where $T(\alpha) = (x'(\alpha), y'(\alpha))$ and $N(\alpha) = (y'(\alpha), -x'(\alpha))$. With this parametrization, we rewrite the integrals with respect to α.

Using this representation of the unknown forces, the derivatives are approximated by the spline coefficients as $Y_i = a_i$, $Y_{si} = b_i, Y_{ssi} = 2c_i$. Recall that the number of unknowns reduces to a_i by using $b = Ba$ and $c = Ca$ with matrices B and C defined by the periodic spline conditions. Therefore, when constructing the matrix $(SD)^*$ as in (50), Eqs. (52) and (55), for example, will form diagonal blocks, whereas equations such as (51), (53), (54) and (56) include terms with spline coefficients b_i and c_i. These will form near diagonal block matrices with coefficients of a_i. Other approximations of the

Table 1
Stokes problem: number of GMRES iterations.

N	No corrections, no preconditioner	Corrected, no preconditioner	Corrected, no preconditioner
168	242	78	24
328	456	110	31
648	950	152	36
1288	2008	212	42

derivatives are possible, and we later compare results using splines and finite differences for the coefficients of Y_s and Y_{ss} to compute the matrix $(SD)^*$.

5.3. Stokes problem

In Section 4.1, we have introduced the preconditioner for the Stokes problem. Here we illustrate the efficiency of GMRES when applying this preconditioner. We solve the following problem: compute Stokes flow in $\Omega_S = (0,1)\times(1,2)$ using the boundary condition

$$\mathbf{u}_S = (0, x(x-1)), \quad \mathbf{x}\in\partial\Omega_S.$$

We assume viscosity $\mu = 1$ and discretize the boundary using N points. The systems have dimensions $2N\times 2N$. Table 1 compares how the number of GMRES iterations grows with the matrix size, where the tolerance was kept fixed at 10^{-7}. We observe that the number of iterations using the peconditioner is significantly reduced, and although still growing as the matrix size increases, the growth rate is much slower compared with the matrix without preconditioner. Similar results were obtained in the Darcy framework, which demonstrates that this preconditioner could be applied to Stokes and Darcy problems separately.

5.4. Coupled problem

The matrix in the previous example corresponds to $\mathcal{K}^{\mathbf{u}}_{\delta c}$ in the system (41). Although the Stokes problem alone is simpler to analyze, we expect the same kind of improvement of GMRES for the coupled system (41). Consider Darcy flow in $0\leqslant x\leqslant 1, 0\leqslant y\leqslant 1$ and Stokes flow in $0\leqslant x\leqslant 1, 1\leqslant y\leqslant 2$, satisfying continuity of normal components of velocity and normal stress and the no-slip condition ($\gamma=\infty$) along the interface $y=1$. The case with a non-zero slip will give similar results. The exact solution is

$$\begin{aligned}
p_D &= \frac{\mu}{k}\left[x(1-x)(y-1)+\frac{(y-1)^3}{3}\right]+2\mu,\\
\mathbf{u}_D &= ((2x-1)(y-1), x(x-1)-(y-1)^2),\\
p_S &= 2\mu y,\\
\mathbf{u}_S &= (0, x(x-1)).
\end{aligned}$$

We use this solution to assign the velocity along the outer Stokes boundary and pressure along the outer Darcy boundary. The numerical solution of this problem was presented in [34].

5.4.1. Dependence on the discretization and regularization parameters

In this section, we fix viscosity $\mu = 1$, permeability $k = 1$, and analyze the convergence properties of the iterative scheme for different discretization Δs and regularization δ values. Each boundary is discretized using N points. Then the matrix that results from imposing the boundary conditions has dimensions $3N\times 3N$, since there are $2N$ unknowns for Stokes forces and N unknowns for Darcy. It should be noted here that while using regularization $\delta/\Delta s$ for Stokes, we use a higher regularization $\delta/\Delta s+2$ for Darcy, since the kernels in Darcy integrals are more singular and thus require stronger smoothing in practice [34]. The system is solved using restarted GMRES [30] with the restart value denoted here by N_Krylov and a given tolerance for the residual.

We first solve the system (41) without preconditioner. Figs. 3 and 4 show the eigenvalues of the matrix for $N = 328$ points on each boundary, so that $\Delta\alpha = \Delta s \approx 0.0122$. The optimal regularization $\delta/\Delta s = 1$ for Stokes and $\delta/\Delta s + 2$ for Darcy was used. The system is not well-conditioned and most of the eigenvalues being near zero is reflected in slow convergence of the iterative method (Table 2).

Table 2 shows condition numbers of matrices and convergence rates of GMRES with tolerance fixed at 10^{-9}. The notation cond # S (respectively cond # D) indicates the condition numbers for Stokes part of the system solved with boundary conditions (3), (6) and (7) (respectively Darcy part with the boundary conditions (4) and (5)). This test shows that although the two problems separately do not have good condition numbers, this conditioning becomes significantly worse when coupling them. We roughly double the number of points on the boundary each time, also decreasing regularization while keeping the

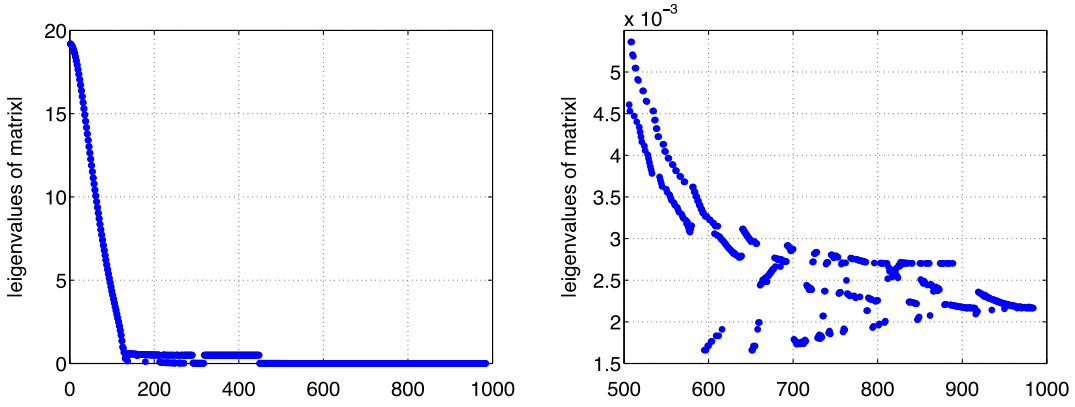

Fig. 3. Coupled system: matrix without preconditioner. Right: close-up of the smallest eigenvalues.

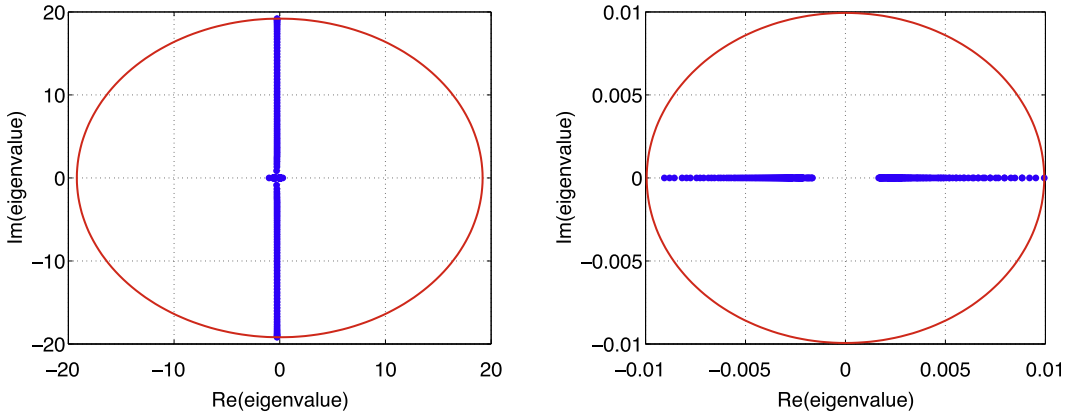

Fig. 4. Coupled system: matrix without preconditioner. Right: close-up of the smallest eigenvalues.

Table 2
Coupled system: convergence for various grid sizes.

Without preconditioner						With preconditioner			
N	cond # S	cond # D	cond # S–D	N_Krylov	GMRES iter	*N*	cond # S–D	N_Krylov	GMRES iter
168	1.96×10^2	1.78×10^3	1.18×10^5	200 250	5000+ 226	168	2.43×10^2	50 100	5000+ 54
328	3.87×10^2	3.88×10^3	4.61×10^5	350 500	5000+ 351	328	$6.56^{\times}10^2$	100	66
648	7.68×10^2	8.18×10^3	1.82×10^6	500 1000	5000+ 550	648	1.84×10^3	500	83
1288	1.53×10^3	1.72×10^4	7.20×10^6	3500	888	1288	5.23×10^3	1000	102

ratio $\delta/\Delta s$ fixed. As we can observe, refining the boundary discretization impairs these numbers, so that condition numbers grow roughly quadratically. For each N, there is a considerable reduction in the condition numbers when using preconditioners. Comparing the cond # S–D and N_Krylov columns in the corresponding tables, it is obvious that the preconditioned matrix not only converges much faster than the original one, but does so with a smaller restart value N_Krylov, which makes the algorithm even more robust. For instance, for the 504×504 matrix ($N = 168$), the algorithm without preconditioner converges in 226 iterations, but N_Krylov of at least 250 is required for convergence. In the preconditioned case however, the algorithm converges in only 54 iterations. Doubling the matrix dimension results in 351 iterations with a roughly doubled N_Krylov in the original calculations, whereas the preconditioned system converges in only 66 iterations, which was possible to obtain without increasing the Krylov subspace dimension.

The eigenvalues of the preconditioned matrix, shown for the case $N = 328$ in Fig. 5, have a smaller spectrum than the eigenvalues of the original matrix (Fig. 4), since applying the preconditioner seems to keep the largest eigenvalue bounded, and the smaller eigenvalues are not as near zero. Table 3 shows the largest and the smallest eigenvalues of the matrices for

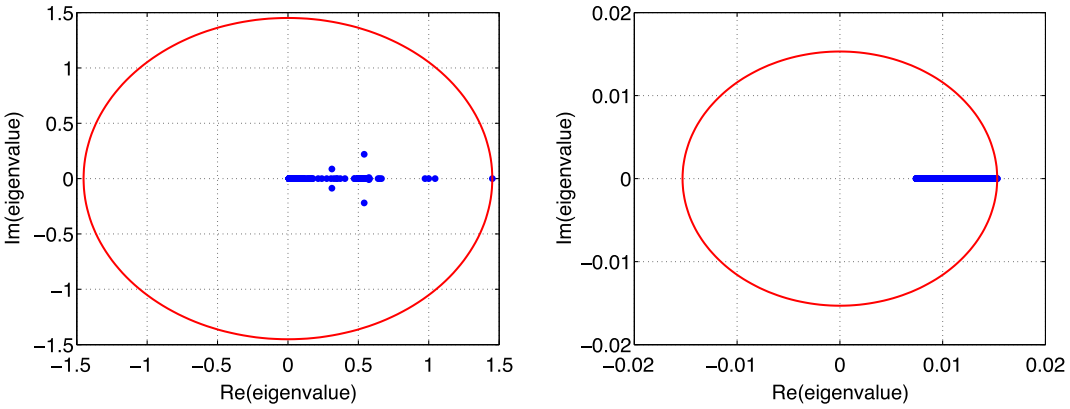

Fig. 5. Coupled system: matrix with preconditioner. Right: close-up of the smallest eigenvalues.

Table 3
Coupled system: eigenvalue range for various grid sizes.

N	Without preconditioner			With preconditioner		
	cond #	$\lvert\lambda_{min}\rvert$	$\lvert\lambda_{max}\rvert$	cond #	$\lvert\lambda_{min}\rvert$	$\lvert\lambda_{max}\rvert$
168	1.18×10^5	0.0033	13.7122	2.43×10^2	0.0145	1.4544
328	4.61×10^5	0.0017	19.1950	6.56×10^2	0.0074	1.4543
648	1.82×10^6	0.0008	26.9959	1.84×10^3	0.0038	1.4543
1288	7.20×10^6	0.0004	38.0665	5.23×10^3	0.0019	1.4542

different N. In the preconditioned case, the largest eigenvalue remains fixed. For the original matrix, the eigenvalue is growing with the matrix size. The smallest eigenvalue, on the other hand, is being halved each time we double the number of points in both cases. However, without using the preconditioner, they are closer to zero.

The next numerical experiments demonstrate the effect of regularization on convergence properties. We keep the discretization fixed at $N = 328$, and vary the regularization by changing the ratio $\delta/\Delta s$. Table 4 shows condition numbers and the eigenvalue range of the matrix system. If we do not use preconditioner, for all values of δ, the condition numbers are of the order of 10^5. Applying the preconditioner reduces the condition numbers significantly. An important observation is that the largest eigenvalue in magnitude is growing for larger δ without the preconditioner, but in the preconditioned case it remains bounded. The smallest eigenvalue $|\lambda_{min}|$ is closer to zero without preconditioner. We observe that the number of iterations decreases when increasing the regularization parameter, while the eigenvalues increase in magnitude, see the $|\lambda_{min}|$ and $|\lambda_{max}|$ columns in Table 4.

5.4.2. Dependence on the physical parameters

In this section, we investigate how the convergence of the iterative method depends on values of the fluid viscosity μ and the permeability of the porous medium k, which can differ by orders of magnitude in practice. This results in different blocks of system (41) having different scales, which may affect the convergence. We investigate this by fixing μ, and varying k. We use the same geometry and same example as before, $N = 328, \delta/\Delta s = 1$ for Stokes and $\delta/\Delta s + 2$ for Darcy, GMRES with a tolerance 10^{-5}, N_Krylov = 500 without preconditioner, and N_Krylov = 100 with preconditioner. Table 5 shows results with

Table 4
Coupled system: convergence for various regularization parameters.

$\delta/\Delta s$	Without preconditioner				With preconditioner			
	cond #	$\lvert\lambda_{min}\rvert$	$\lvert\lambda_{max}\rvert$	GMRES iter	cond #	$\lvert\lambda_{min}\rvert$	$\lvert\lambda_{max}\rvert$	GMRES iter
1.0	4.61×10^5	0.0017	19.1950	351	6.56×10^2	0.0074	1.4543	66
1.5	3.73×10^5	0.0023	20.7322	324	4.63×10^2	0.0117	1.4544	59
2.0	3.21×10^5	0.0031	22.1642	307	4.20×10^2	0.0156	1.4544	54
2.5	2.90×10^5	0.0038	23.5098	292	3.85×10^2	0.0195	1.4544	50
3.0	2.69×10^5	0.0046	24.7832	283	3.57×10^2	0.0235	1.4544	48
3.5	2.53×10^5	0.0053	25.9952	273	3.33×10^2	0.0274	1.4544	45
4.0	2.42×10^5	0.0061	27.1542	267	3.12×10^2	0.0314	1.4544	44

Table 5
Coupled system: convergence rates for different physical parameters.

μ	k	Without preconditioner		With preconditioner	
		cond #	GMRES iter	cond #	GMRES iter
1	1	4.61×10^5	259	6.56×10^2	40
	10^{-1}	4.61×10^4	259	5.47×10^2	41
	10^{-2}	4.62×10^3	264	3.08×10^2	42
	10^{-4}	1.26×10^4	231	3.63×10^3	51
10^{-2}	1	5.08×10^5	192	6.56×10^2	26
	10^{-1}	5.10×10^4	196	5.47×10^2	27
	10^{-2}	5.40×10^3	202	3.08×10^2	29
	10^{-4}	3.93×10^3	198	3.63×10^3	39
10^2	1	4.62×10^5	316	6.56×10^2	53
	10^{-1}	6.61×10^4	312	5.47×10^2	53
	10^{-2}	6.61×10^4	316	3.08×10^2	55
	10^{-4}	1.26×10^6	281	3.63×10^3	64

$\mu = 1, 10^{-2}$, and 10^2, and varying k. Although the number of iterations is still dependent on the parameter values, we again observe that the preconditioner improves the convergence of GMRES in each case.

5.5. Coupled problem on a larger domain

The geometry in the preceding example is represented by unit squares for both Stokes and Darcy flows. Here we repeat the test of Section 5.4.1 on a bigger rectangular geometry: $0 \leqslant x \leqslant 2.5, -1 \leqslant y \leqslant 1$ for Darcy and $0 \leqslant x \leqslant 2.5, 1 \leqslant y \leqslant 3$ for Stokes domains. Table 6 shows the condition numbers and the number of GMRES iterations with N_Krylov = 2000 and tolerance fixed at 10^{-9}, with $N_0 = 378$ points along the boundary of each domain. As before, we see a reduction in matrix condition numbers of at least two orders of magnitude, and convergence is significantly improved. Notice that the speed-up between iteration numbers grows from 4 in the first to 8 in the last case.

5.6. Another geometry

In this section, we present an example where the interface between Stokes and Darcy domains is not a straight line. The geometry is given in Fig. 6, where $\bar{\Omega}_S = [-1.5, 1.5] \times [-1.5, 1.5] \setminus \Omega_D$, and the interface Σ is parametrized by $x = 0.7(\cos(t) + 0.4\cos(2t)) - 0.2, y = 0.7\sin(t), 0 \leqslant t \leqslant 2\pi$. Along the outer Stokes boundary Γ_S, we impose $\mathbf{u}_S = (0, 4 - x^2)$ as a boundary condition. Parameter values $\mu = 1, k = 1, \gamma = \infty$, regularization $\delta/\Delta s = 1$ for Stokes and $\delta/\Delta s + 2$ for Darcy, and tolerance = 10^{-9} for GMRES were used in the calculations. The matrix condition numbers and GMRES iteration numbers are shown in Table 7. By N_0 we indicate the case with 220 points along the interface Σ and 504 points along the outer Stokes boundary Γ_S.

The preconditioner improved the iteration numbers significantly. Indeed, the system for $4N_0$ does not converge to the desired tolerance in 5000 iterations, whereas with preconditioner it only takes 390 iterations. We modified N_Krylov = 5000 and tolerance 10^{-5} (last row in Table 7). In this case, the tolerance was attained after 2158 iterations, and only 244 with preconditioner.

5.7. Finite difference approximation of derivatives

All the results above use coefficients of cubic splines to approximate the derivatives of forces. This results in a preconditioner with blocks that have a few non-zero off-diagonal elements. Alternatively, a different approximation for the derivatives can be used to reduce the block-bandwidth of the preconditioner. In particular, we use second-order finite differences

Table 6
Coupled system: convergence for various grid sizes.

N	Without preconditioner		With preconditioner	
	cond #	GMRES iter	cond #	GMRES iter
N_0	1.19×10^5	422	5.85×10^2	106
$2N_0$	4.85×10^5	695	1.55×10^3	123
$4N_0$	1.95×10^6	1188	4.53×10^3	136

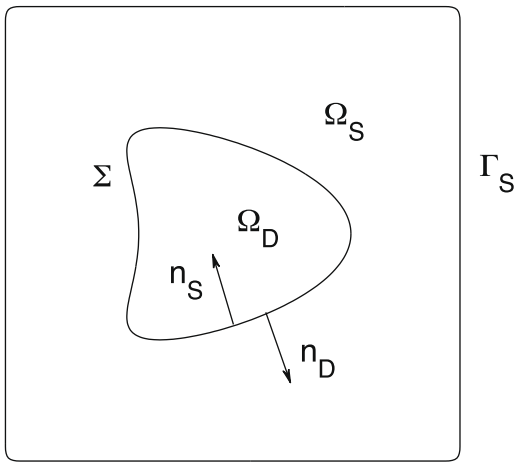

Fig. 6. Geometry of the problem.

Table 7
Coupled system: convergence for various grid sizes.

N	Without preconditioner		With preconditioner	
	cond #	GMRES iter	cond #	GMRES iter
N_0	2.57×10^9	676	3.17×10^7	211
$2N_0$	6.59×10^{11}	2000	3.88×10^9	286
$4N_0$	5.18×10^{13}	5000++	1.50×10^{11}	390
$4N_0$	***	2158	***	244

Table 8
Convergence rates: preconditioners computed with cubic splines vs. finite differences.

k	Cubic splines	Finite diff.	Block-diag. with splines	Without preconditioner
1	40	40	123	259
10^{-1}	41	41	124	259
10^{-2}	42	42	126	264
10^{-4}	51	51	83	231

for f_s, f_{ss}, g_s, and g_{ss}. This way, the blocks of the matrix $(SD)^*$ formed from the coefficients of f and g in (51)–(56) have at most a tridiagonal structure with periodic conditions, and computing the preconditioner becomes cheaper. We repeat the test of Section 5.4, where we fix the viscosity $\mu = 1$ and vary the permeability, comparing results for the two preconditioners. Again, tolerance = 10^{-5} and N_Krylov = 100. As can be seen from Table 8, the GMRES iteration numbers with the preconditioned matrix using cubic splines (which were shown also in Table 5) and using finite differences are identical. This indicates that to construct the preconditioner, any approximation of the derivatives of forces could be used, and should be chosen so that the resulting preconditioner is easier to solve. As a comparison, we also modify the original preconditioner obtained with cubic splines to have a block-diagonal structure. This preconditioner has the simplest structure and therefore is cheapest to solve. We compute it by truncating the off-diagonal elements of the original preconditioner. The results are shown in the fourth column of Table 8. It can be seen that applying this simple preconditioner is already beneficial, it reduces the number of iterations by a factor of two.

6. Conclusions

In this paper, we have introduced a preconditioner to efficiently solve the coupled Stokes–Darcy integral formulation. This boundary integral formulation is obtained through a regularization-correction method. We derived the preconditioner based on the observation that the correction procedure improves condition numbers of the system. Numerical results validate this approach and have shown significant improvement of the Krylov subspace method. Moreover, this preconditioner can be used in systems of integral equations involving the same kind of Green's function, as we showed for a Stokes flow problem.

We also believe that this preconditioner could be extended to integrals with the singular Green's function (without regularization-correction).

The preconditioner proposed in this work can be solved efficiently since it has a small bandwidth. Indeed, the blocks of this matrix are either diagonal or have only a few non-zero off-diagonal elements obtained because of the approximation of the derivatives on the densities. The approach used in this work to approximate these derivatives is cubic splines. However, to reduce the number of off-diagonal elements we also performed numerical differentiation using finite differences. In both cases, we observe that the preconditioner has the same effect on the iterative method.

References

[1] J. Ainley, S. Durkin, R. Embid, P. Boindala, R. Cortez, The method of images for regularized Stokeslets, J. Comput. Phys. 227 (9) (2008) 4600–4616.
[2] K.E. Atkinson, The Numerical Solution of Integral Equations of the Second Kind, Cambridge University Press, Cambridge, 1997.
[3] J.T. Beale, M.C. Lai, A method for computing nearly singular integrals, SIAM J. Numer. Anal. 38 (2001) 1902–1925.
[4] J.T. Beale, A.T. Layton, On the accuracy of finite difference methods for elliptic problems with interfaces, Commun. Appl. Math. Comput. Sci. 1 (2006) 91–119.
[5] J. Bear, A. Verruijt, Modeling Groundwater Flow and Pollution, Riedel Publishing, 1987.
[6] G.S. Beavers, D.D. Joseph, Boundary conditions at a naturally permeable wall, J. Fluid Mech. 30 (1967) 197–207.
[7] E. Burman, P. Hansbo, A unified stabilized method for Stokes' and Darcy's equations, J. Comput. Appl. Math. 198 (2007) 35–51.
[8] D. Colton, R. Kress, Inverse Acoustic and Electromagnetic Scattering Theory, second ed., Springer-Verlag, Berlin, 1998.
[9] R. Cortez, The method of regularized Stokeslets, SIAM J. Sci. Comput. 23 (4) (2001) 1204–1225.
[10] R. Cortez, L. Fauci, A. Medovikov, The method of regularized Stokeslets in three dimensions: analysis, validation, and application to helical swimming, Phys. Fluid 17 (2005) 1–14.
[11] M. Discacciati, E. Miglio, A. Quarteroni, Mathematical and numerical models for coupling surface and groundwater flows, Appl. Numer. Math. 43 (2002) 57–74.
[12] M. Discacciati, A. Quarteroni, A. Valli, Robin–Robin domain decomposition methods for the Stokes–Darcy coupling, SIAM J. Numer. Anal. 45 (3) (2007) 1246–1268.
[13] H. Flores, E. Lobaton, S. Méndez-Diez, S. Tlupova, R. Cortez, A study of bacterial flagellar bundling, Bull. Math. Biol. 67 (2005) 137–168.
[14] J. Galvis, M. Sarkis, Balancing domain decomposition methods for mortar coupling Stokes–Darcy systems, Lect. Note Computat. Sci. Eng. (2006).
[15] L. Greengard, M.C. Kropinski, A. Mayo, Integral equation methods for Stokes flow and isotropic elasticity in the plane, J. Comput. Phys. 125 (1996) 403–414.
[16] L. Greengard, M.C. Kropinski, Integral equation methods for Stokes flow in doubly-periodic domains, J. Eng. Math. 48 (2004) 157–170.
[17] J.K. Guest, J.H. Prevost, Topology optimization of creeping fluid flows using a Darcy–Stokes finite element, Int. J. Numer. Meth. Eng. 66 (2006) 461–484.
[18] J. Helsing, R. Ojala, On the evaluation of layer potentials close to their sources, J. Comput. Phys. 227 (2008) 2899–2921.
[19] G.C. Hsiao, W.L. Wendland, Boundary Integral Equations, first ed., Springer-Verlag, Berlin, 2008.
[20] W. Jager, A. Mikelić, On the boundary conditions at the contact interface between a porous medium and a free fluid, Ann. Scuola Norm. Sup. Pisa Cl. Sci. 23 (1996) 403–465.
[21] W. Jager, A. Mikelić, On the interface boundary condition of Beavers, Joseph, and Saffman, SIAM J. Appl. Math. 60 (2000) 1111–1127.
[22] R. Kress, Linear Integral Equations, second ed., Springer-Verlag, New York, 1999.
[23] W.J. Layton, F. Schieweck, I. Yotov, Coupling fluid flow with porous media flow, SIAM J. Numer. Anal. 40 (6) (2003) 2195–2218.
[24] K.A. Mardal, X.-C. Tai, R. Winther, A robust finite element method for Darcy–Stokes flow, SIAM J. Numer. Anal. 40 (2002) 1605–1631.
[25] A. Masud, T.J.R. Hughes, A stabilized mixed finite element method for Darcy flow, Comput. Meth. Appl. Mech. Eng. 191 (2002) 4341–4370.
[26] C.S. Peskin, B.F. Printz, Improved volume conservation in the computation of flows with immersed elastic boundaries, J. Comput. Phys. 105 (1993) 33–46.
[27] O.M. Phillips, Flow and Reactions in Permeable Rocks, Cambridge University Press, Cambridge, 1991.
[28] C. Pozrikidis, Boundary Integral and Singularity Methods for Linearized Viscous Flow, Cambridge University Press, Cambridge, 1992.
[29] C. Pozrikidis, D.A. Farrow, A model for fluid flow in solid tumors, Ann. Biomed. Eng. 31 (2003) 181–194.
[30] Y. Saad, Iterative Methods for Sparse Linear Systems, second ed., SIAM, 2003.
[31] P.G. Saffman, On the boundary condition at the surface of a porous medium, Stud. Appl. Math. L (2) (1971) 93–101.
[32] M. Sahraoui, M. Kaviany, Slip and no-slip velocity boundary conditions at interface of porous, plain media, Int. J. Heat Mass Transfer 35 (1992) 927–943.
[33] S. Tlupova, Improved accuracy of numerical solutions of coupled Stokes and Darcy flows based on boundary integrals, Ph.D. Thesis, Tulane University, 2007.
[34] S. Tlupova, R. Cortez, Boundary integral solutions of coupled Stokes and Darcy flows, J. Comput. Phys. 228 (1) (2009) 158–179.